acoustics

MDPI

Article

The Recycling and Reuse of Natural Materials: Sound Absorbing Box Patterns That Use Waste from Olive Tree Pruning

Rossella Cottone [1], Louena Shtrepi [1,*], Valentina Serra [1] and Simonetta Lucia Pagliolico [2]

[1] Department of Energy, Politecnico di Torino, Corso Duca Degli Abruzzi 24, 10129 Torino, Italy
[2] Department of Applied Science and Technology, Politecnico di Torino, Corso Duca Degli Abruzzi 24, 10129 Torino, Italy
* Correspondence: louena.shtrepi@polito.it

Abstract: The agricultural activity of pruning olive trees generates waste which, due to long-standing practices and unawareness of the consequences, are burned on site, thereby producing CO_2 emissions in the atmosphere. Therefore, in order to prevent environmental pollution and a waste of resources, the aim of this research investigation was to highlight some alternative uses of the pruning of olive trees waste. This work focuses on recycled and reused by-products as a secondary raw material for the implementation of interior components that can be used for indoor acoustic correction purposes and evaluates their potential as absorbing materials, without overlooking the aesthetic dimension. In this paper, different configurations based on plywood frames with loose olive pruning chips used as a filler, namely, modules and sub-modules, were investigated. Moreover, other technological details, that is, the influence of a Tissue-Non-Tissue (TNT) layer and a spray film coating applied over the external surface of the loose material, were measured. Sound absorption measurements were conducted inside a small-scale reverberation room (SSRR) and the experimental results demonstrated that the samples, for the given thickness, have weighted sound absorption values (α_w) of between 0.15 and 0.35 and single third-octave band values that can reach higher values than 0.50 above 500 Hz. The frequency curves and weighted values of the samples in which the influence of TNT and the spray film coating were tested remained unchanged. This is a design aspect that allows absorbing surfaces to be modeled and integrated with existing walls, while maintaining the acoustic performance and the specific aesthetic features of the loose material.

Keywords: agricultural waste; sound absorption; natural materials; raw material; acoustical performance; small-scaled reverberation room; plywood frames design

Citation: Cottone, R.; Shtrepi, L.; Serra, V.; Pagliolico, S.L. The Recycling and Reuse of Natural Materials: Sound Absorbing Box Patterns That Use Waste from Olive Tree Pruning. *Acoustics* **2023**, *5*, 177–192. https://doi.org/10.3390/acoustics5010011

Academic Editor: Patrizio Fausti

Received: 24 December 2022
Revised: 25 January 2023
Accepted: 1 February 2023
Published: 5 February 2023

1. Introduction

In recent years, natural materials have become increasingly close in performance to traditional sound absorption surface treatments, which are obtained through the use of synthetic fibers, but with significantly reduced production costs, improved biodegradability, light weight [1], and a lower environmental impact than more conventional materials [2].

However, despite the broad research on the subject, there are still very few studies on some of the natural fibers or agricultural by-products, e.g., olive tree related materials, that can be used as acoustically absorbent materials.

Because of the ongoing climate change and the global environmental crisis, attention is now being paid to the use of natural fibers, especially recycled fibers, as sound absorbing materials. The Life Cycle Assessment (LCA) study conducted by Asdrubali et al. [3] found that the production of synthetic materials requires a large amount of energy during the production cycle, which leads to a worsening of the current climate conditions. Natural materials instead help reduce the carbon footprint, because their production does not rely on the use of chemicals and they consume less energy and fewer fossil fuels.

Berardi and Iannace [4,5] examined the acoustic properties of natural materials by measuring the sound absorption coefficient of multiple fibers, including kenaf, wood, mineralized wood, hemp, coconut, cork, water reed bark and wood, and sheep wool. The measurements made by the research team confirmed that these materials are good absorbers, especially at medium and high sound frequencies, often even without the addition of a binder, and higher absorption values were obtained for increased thicknesses of the material.

The research conducted by Bousshine et al. [6] involved the acoustic characterization, in the 200–1400 Hz frequency band, of other sustainable materials derived from plants, agricultural and animal waste, such as date palm (trunk, petiole, pinnate leaves, cluster and fiber net), cane, esparto, olive leaves, fig branches, wood sawdust, chicken feathers, and sheep wool. The results showed that these materials can offer a good acoustic performance, with absorption coefficients in the 0.6–0.9 range at medium frequencies. Moreover, petiole, esparto, wood sawdust, sheep wool, and chicken feathers showed similar absorption capacities to glass wool up to 600 Hz, thus indicating that these materials can be considered promising sound absorbers that could play important roles in acoustic correction methods. Olive leaves, in particular, showed a better absorption at medium frequencies, with a maximum of about 0.98 close to the 520 Hz frequency. However, the absorption coefficient decreased, beyond the maximum values, to a minimum of about 0.62. The sound absorption of the leaves remained acceptable at high frequencies. The same authors carried out research [7] on the same materials, albeit wetted with water, to obtain a bound paste that was formed by mixing them with 60 percent recycled cardboard. In this case, the acoustic absorption of the olive leaves remained acceptable, that is, above 0.4, over the entire 200–1400 Hz frequency range.

Many of these materials were also analyzed in [8–12]. Arenas et al. [12] carried out a study on three different types of loose esparto (originating from Pakistan, Tunisia, and Egypt), without the addition of chemicals or binders. The three materials showed the characteristic behavior of a porous sound absorbing material, in which the sound absorption coefficient increased with the frequency, and an increase in low-frequency sound absorption was also observed as the material thickness increased. Another loose material that has demonstrated interesting sound absorption properties is bamboo. Putra et al. [13] conducted sound absorption coefficient measurements to study the effect of the length and diameter of the stem and of the different arrangements of the bamboo structures with respect to incident sound. The different arrangements led to absorption coefficient peaks above 0.8 for specific frequencies.

Martellotta et al. [14] also studied olive leaves, differentiating between three different grain sizes and comparing loose leaves with leaves bound with chitosan. The samples showed the same behavior up to 400 Hz, with an α of about 0.3. Instead, substantial differences appeared between the samples at higher frequencies, and α increased to values of between 0.55 and 0.95, with maxima at about 1200 Hz and 4000 Hz, and minimum at 2000 Hz.

Given the positive outcomes of such studies, this paper investigates the reuse of olive tree branches and leaves from pruning in sound absorbing structures, thereby promoting a circular economy [15]. The material used for this activity came from Sicily, but the results are of interest to all the Mediterranean areas that have a substantial number of olive groves, since a large amount of waste is generated during pruning and, in most cases, this waste is burned in the fields, thereby producing CO_2 emissions in the atmosphere. For this reason, it would be advantageous to reuse these wastes and convert them into high value-added resources. In this context, Chen et al. [16] also studied the recycling of industrially discarded luffa resources with the aim of preventing environmental pollution caused by their incineration. The research showed that luffa fiber-based sound absorbing composite products have good sound absorption, hygroscopic, and thermal performances, and the average sound absorption coefficient of the considered luffa fiber composite reached 0.65, thereby proving it was a highly efficient sound-absorbing material.

The aim of this research was to connect architecture, innovation, and sustainability by focusing on the recycling of olive tree pruning waste in the building–architectural field. This material has never been fully characterized before by taking into account its aesthetic design value, except for in a few studies in which only differentiated olive leaves or wood were examined considering traditional measurements based on the impedance tube approach [6,14]. In this study, a small-scale reverberation room (SSRR) was used to allow several design configurations to be investigated [17]. Thus, the potential of the materials and components derived from olive tree pruning chips was investigated for application in construction and architecture through the evaluation of their acoustic and aesthetic performance. This latter aspect should not be underestimated, because a sound-absorbing component can have an aesthetic appeal for indoor applications and affect the perception of the indoor environmental quality in general [18]. Moreover, the acoustics community might be interested in having another sustainable decorative type of sound absorber that could have different acoustic performances when arranged in different patterns. It has in fact been shown that using different patterns can significantly affect the acoustic parameters of an indoor space [19,20].

The objective of this paper has been to provide a new perspective, with respect to the normal applications of sound absorbing panels used for the acoustic correction of rooms, by promoting the use of natural loose material. Thus, in order to obtain a more sustainable approach, the loose material was placed inside modular frames, without the use of glues or adhesives, with the aim of excluding the phase of the production cycle related to bonding chips. The final output consisted of box-shaped panels that contained olive wood pruning scraps, in the form of chips of different sizes, which acted as porous sound-absorbing materials.

2. Materials and Methods

The research was designed and developed through the following stages:

(1) Searching for the agricultural by-product obtained from pruning wood chips.
(2) Realization of test specimens and their decomposition into smaller units that hereinafter are referred to as "modules" and "sub-modules", respectively.
(3) Measurement of the sound absorption in the small-scale reverberation room (SSRR) [17] and evaluation of the sensitivity of the absorption coefficients, using the ISO 354 measurement method [21], by varying the position of the test specimens on the floor. The analyzed samples were differentiated into configurations characterized by the composition of the sub-modules, namely, BASE, B_{empty}, B_{full}, $B_{full,1}$, $B_{full,2}$, $B_{full,3}$, B + $O100l_{full}$, and $O100l_{full}$.
(4) Evaluation of the effect of the application of two technological solutions that would improve the fixation of the loose material. A white Tissue-Non-Tissue (TNT) (17 g/m^2) layer was considered as a material to be interposed between loose sound-absorbing wood chips to cover panels, and a spray coating film (tesa®® 60021 Permanent spray glue) was applied as a membrane containment to keep the chips in place and make them visible when the open module was hung in a vertical position.
(5) Computation of the single number indices, that is, the weighted sound absorption coefficients (α_w), as a unique comparative value.

2.1. By-Product of Olive Tree Pruning Wood Chips

The first stage consisted in sourcing, chipping, and selecting the chip size, and then in drying the secondary raw material obtained from olive tree prunings. For this purpose, the material was obtained from the Sicilian territory from the manual production pruning of the Cerasuola cultivar, one of the oldest cultivars in Western Sicily.

Pruned branches and leaves were transformed by means of a tractor-driven chipper with an autonomous motor, into the intermediate product, which consisted of chips of variable-size (Figure 1). The wood chips were first sieved to remove the coarser fraction, and a large chips size (d) between 4 and 10 mm (Table 1) was obtained. The graded olive

wood chips were then placed in a ventilated kiln, set at 103°, to achieve a normal moisture content and a density of around 280 ± 12 kg/m^3.

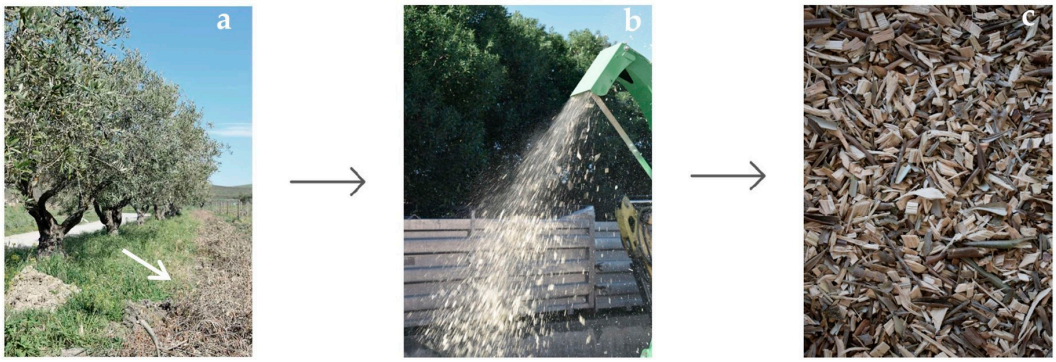

Figure 1. Sequence adopted to obtain the by-product from olive tree pruning: (**a**) pruning product (from pruning waste left on the fields); (**b**) pruning chipping; (**c**) obtained by-product.

Table 1. Characteristics of the basic module.

Sample	External Dimensions of the Module (mm)	Internal Dimensions of the Module (mm)	Maximum Chips Size (mm)	Density of the Loose Material (kg/m^3)	Porosity (%)
O100l	300 × 300 × 44	288 × 288 × 38	4 < d < 10	280 ± 12	68.2

The bulk density of loose-fill chips at normal moisture content (12%) has been calculated as follows: (1) the measuring vessel used was made up of a plywood frame with a base having an internal volume of 288 × 288 × 38 mm^3; (2) after weighing, the frame was filled with an excess amount of loose olive wood chips to form a cone; (3) the bulk material was leveled to the maximum height of the frame (38 mm); (4) the loose chips were settled inside the vessel by hitting it three times on the ground and after each settlement more loose material was added up to the maximum height of the frame; (5) the full frame was weighed; (6) the value of the weight of the loose chips was obtained as the difference between the two weighted values; (7) the bulk density of the loose chips was estimated for three samples as the ratio between the weight of the chips and the internal volume of the frame. The average value of the bulk density was equal to 280 ± 12 kg/m^3. This value was found to be of the same order of magnitude as the bulk density of forest chips found in the literature [22]. This same procedure was used to create the samples described in the following section (Section 2.2). After this phase, the pruning by-product and olive leaves were used to prepare the samples for the acoustic characterization tests.

2.2. Preparation of the Test Specimens

The loose olive tree pruning chips were used, without any binder, to fully fill 300 × 300 × 44 mm birch plywood frames (Figure 2), which constituted the basic module. A birch plywood box was constructed with wood processing waste of a thickness of 6 mm. Thus, the thickness of the cavity filled with loose olive tree pruning chips was equal to d = 38 mm. The basic module was labeled with the initialism O100l, to indicate a composition of 100% loose olive tree pruning chips.

Based on the available data, the porosity ϕ [23] of the sample was calculated from the relation $\phi = 1 - (\rho_b/\rho_s)$, where ρ_b is the bulk density of the loose-fill olive wood chips (280 ± 12 kg/m^3) and ρ_s is the apparent density of the solid olive wood (880 kg/m^3), as found in the literature [24]. A porosity of about 68.2% was estimated. However, further detailed studies could be conducted to obtain a more accurate estimation with experimental measurements.

The overall characteristics of O100l are summarized in Table 1.

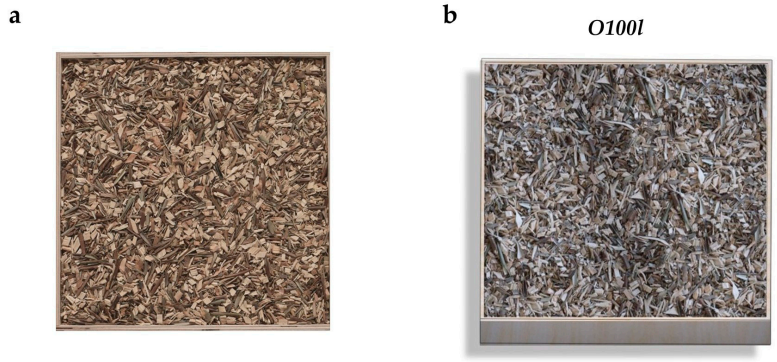

Figure 2. (**a**) Photo of the sample; (**b**) 3D image of a frame containing loose chips.

2.2.1. Design of the Samples in Different Pattern Configurations

Sixteen differently shaped sub modules were made using the same material and with the same frame thickness and were used in different configurations inside the frame of the basic module. Figure 3 shows the sizes of the sub-modules, which are differentiated into black, gray, and white colors according to their maximum size. Specifically, the maximum base dimensions, 300 × 300 mm, are shown in black; the dimensions adopted for the decomposition of the base frames into 200 × 200 mm are shown in gray; and the dimensions considered for a further decomposition, 100 × 100 mm, are shown in white.

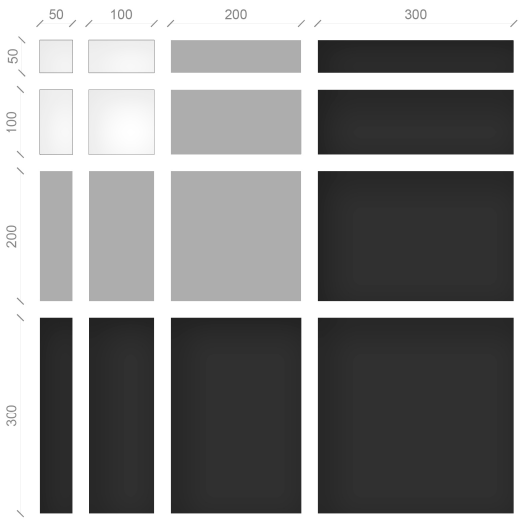

Figure 3. 2D modeling of the sub-module frames by decomposition. The basic module is shown in black 300 x 300 mm. Sub-modules with maximum base dimensions of 200 mm by 200 mm are shown in gray and those with maximum base dimensions of 100 mm by 100 mm are shown in white.

The objective of this phase was to stimulate the flexibility and customization of environmental surfaces, as these sub-modules could be composed together, like a Mondrian painting, or like a puzzle, by adding and/or subtracting volumes. This possibility of composition allowed a conspicuous pattern variability to be obtained. Some pattern examples are shown in Figure 4.

Pattern-B was chosen for acoustic characterization because of the dimensional variation of its sub-modules. This pattern allowed more flexibility to be taken into consideration in the combinations of the sub-modules over the reference area (BASE). Different configurations of the pattern were analyzed, with the sides enclosing a base area of 0.27 m^2, by varying the exposed area of the porous material and the position of the individual sub-modules to investigate the effects on the frequency absorption values. The first configuration (Figure 5) represents an acoustically hard base of 6 mm of plywood (BASE); the

second is an empty pattern with the acoustically hard sub-module boxes located in the center of the BASE configuration (B_{empty}); the third is based on the B_{empty} configuration, with the pattern being filled with olive tree pruning wood chips (B_{full}). Finally, five sub-module configurations were differentiated: $B_{full,1}$, $B_{full,2}$, $B_{full,3}$, B + $O100l_{full}$ (B_{full} + 2 full basic O100l modules), and $O100l_{full}$ (3 full basic O100l modules). Figure 6 shows the eight configurations that were analyzed by means of the SSRR method; the positions of the sources, with respect to the individual full or empty frames, can be also deduced.

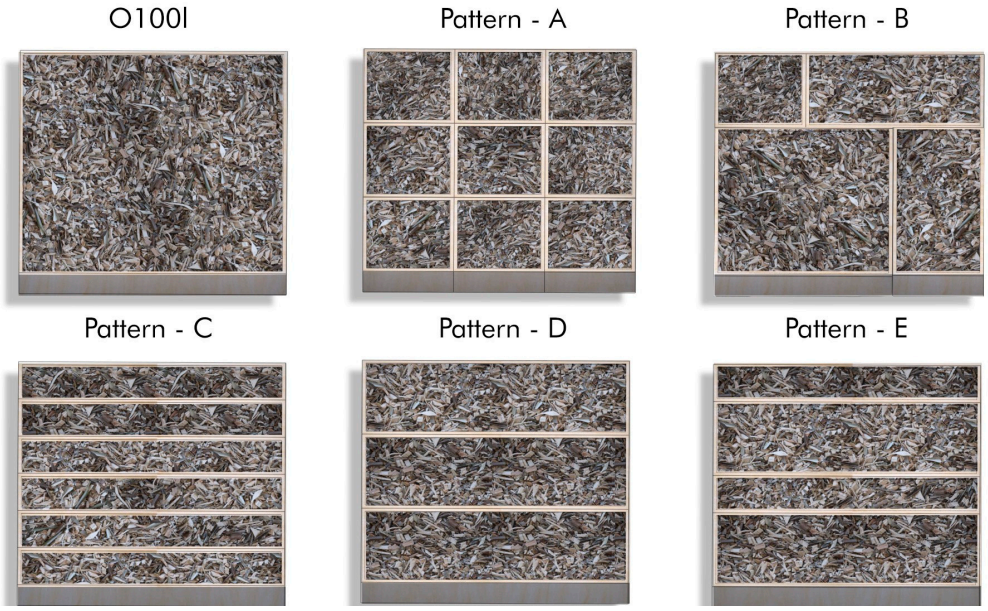

Figure 4. 3D modeling and rendering of the possible patterns composed of the birch plywood frame sub-modules with olive wood chips as the filler material.

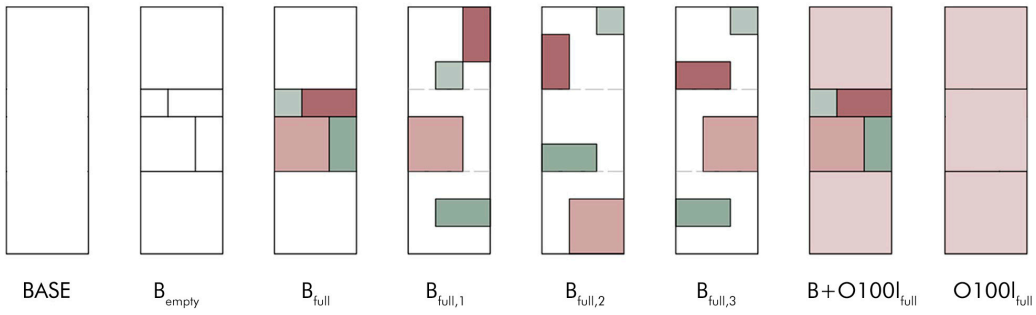

Figure 5. Design configurations of Pattern-B and the basic module of the total area. The Pattern-B is subdivided as follows: the smaller sub-module (light green) is a 100 × 100 mm square; the two rectangular sub-modules (green and red) have the dimensions of 100 × 200 mm; finally, the bigger sub-module is a 200 × 200 mm square.

2.2.2. Surface Treatment: The Use of TNT or a Spray Coating

Two technological solutions, with a surface treatment, were applied so as to use the loose wood chips, without mixing them with binders or adhesives, in the preliminary stage, in order to realize sound-absorbing panels that could be placed on walls in a vertical position.

First, a white TNT wrap (17 g/m^2) was used as a containing layer. The TNT was placed on top of the $O100l_{full}$ configuration (see Figure 7). It is an inexpensive, odorless material, and it is environmentally sustainable as it can be used many times. A white TNT was used for experimental purposes, but various colors of TNT are available to obtain different sound-absorbing configurations (see Figure 8).

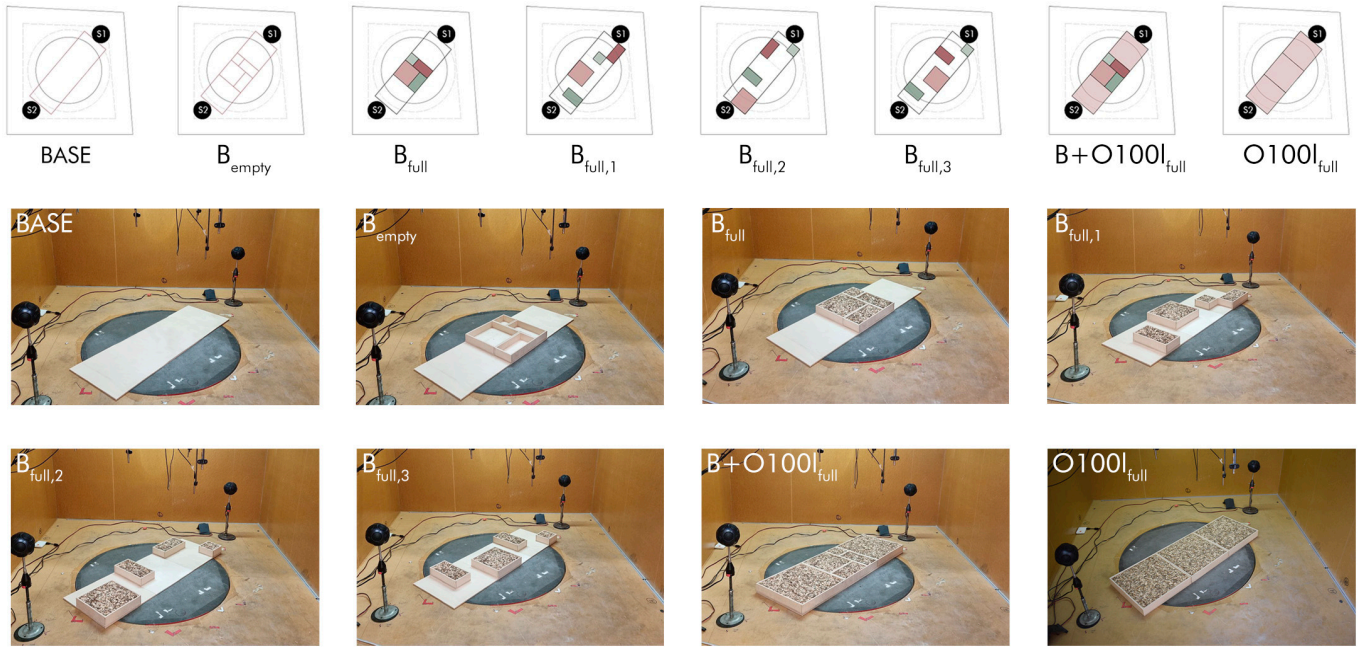

Figure 6. The different configurations of the sub-modules.

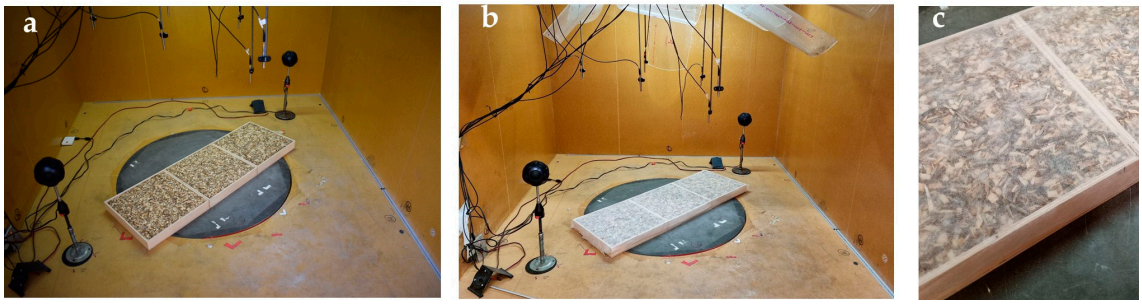

Figure 7. (**a**) O100l$_{full}$ configuration; (**b**) O100l$_{full}$ configuration with TNT; (**c**) details of the TNT.

Figure 8. 3D modeling and rendering of the sound-absorbing panel (O100l$_{full}$ and Pattern-B) with pruning wood chips from of olive trees used as the filling material and TNT as the containing membrane.

As an alternative, the top open base of four sub-modules (B$_{full,2}$ configuration) was sprayed with a silicone-free film coating, based on synthetic rubbers (tesa® 60021 named Spray glue Permanent), to keep the chips in place when the component was hung in a vertical position. It was necessary to wait a few minutes for the spray to dry before performing a new measurement. An enlargement of the surface effect created by the spray on the loose material is shown in Figure 9c.

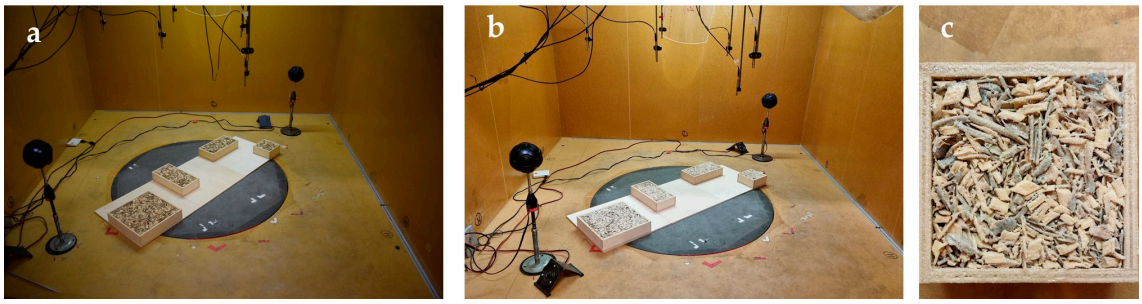

Figure 9. (**a**) $B_{full,2}$ configuration; (**b**) $B_{full,2}$ configuration with a spray film coating; (**c**) details of the sprayed surface.

2.3. Measurement of the Sound Absorption Coefficient

The small-scale reverberation room (SSRR) in the Department of Energy (DENERG) at the Politecnico di Torino was used for the measurement of the sound absorption coefficient, according to the ISO 354:2003 procedure [21] and the ASTM C423 [25] standard. This room is shown in Figure 10a and it was described in detail and validated in [17]. This room is a 1:5 scale reproduction of the Instituto Nazionale di Ricerca Metrologica (INRiM) reverberation room, which requires a sample area of 10 to 12 m^2. Therefore, over the years, a methodology has been sought that is as assimilable and accurate as that of the reverberation room but, at the same time, which has a lower resource and economic consumption. The use of the SSRR allows smaller sample sizes than 10–12 m^2 to be used, but at the same time maintains the diffuse field conditions of the method. However, this methodology suffers from certain disadvantages, such as a lack of field diffusivity in the mid to low frequencies and diffraction due to the finite size of the experimental samples, which generates the so-called edge effects. The SSRR measurement methodology specifically consists of an exponential sweep, from 100 to 25,000 Hz, which is a digital signal that is sent to a sound card, amplified and generated by the omnidirectional dodecahedral sound sources in the room. The microphones record the audio, and the signal is then sent to the used computer. The signal generation and recording operations are carried out twice during a measurement, that is, once for the first source (S1) and once for the second one (S2) (see Figure 10a,b). Measurements are recorded for the six microphone positions for both sources, for a total of twelve measurements, as required by ISO 354. To this aim, the measurement chain consists of six 1/400 BSWA Tech MPA451 microphones and ICP104 (BSWA Technology Co., Ltd., Beijing, China); two ITA High-Frequency Dodecahedron Loudspeakers, with their specific ITA power amplifiers (ITA-RWTH, Aachen, Germany); and a Roland Octa-Capture UA-1010 sound card (Roland Corporation, Osaka, Japan).

MATLAB software, combined with the functions of the ITA-Toolbox (an open-source toolbox from RWTH-Aachen, Aachen, Germany) [26], was used for the measurement of the sound absorption coefficient. The input data that influence the absorption factor of the air inside the room were entered, namely, temperature, relative humidity, and atmospheric pressure. A monitoring sensor, connected directly to the computer, was placed inside the room to consider any variation that could occur to these factors during testing. Using these data made it possible to automatically generate the results of the sound absorption coefficient, as a function of the exposed area of the test sample, and of the sound absorption coefficient of the empty room under the same environmental conditions. A key factor was the size of the sample, whose standard measurements were between 0.40 and 0.48 m^2. In the experimental setup, as anticipated, a reference area of 0.27 m^2 was considered for all the configurations, although it emerged from the studies carried out in [17] that using too small a sample could result in diffraction effects and lower absorption, comparable with those of the empty room.

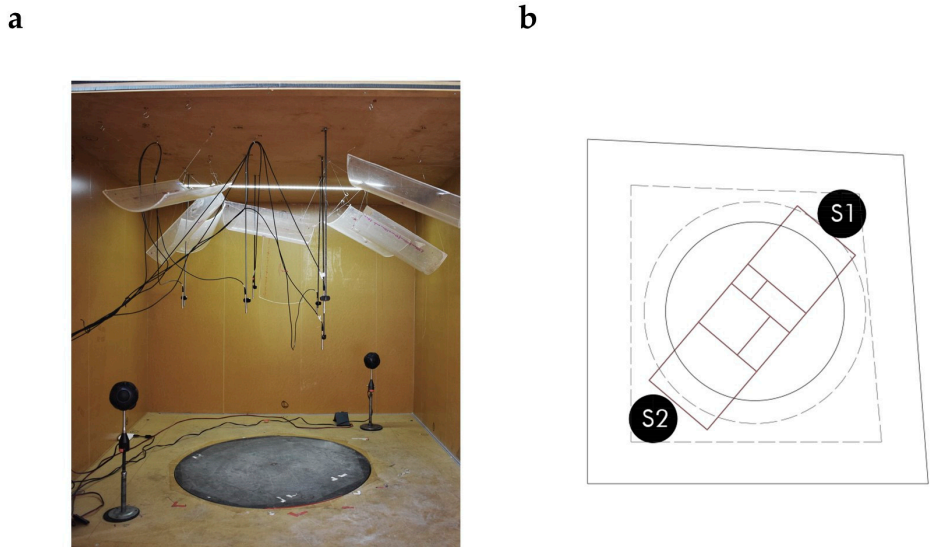

Figure 10. (**a**) Empty small-scale reverberation room; (**b**) example of the configuration of the SSRR floor plan, with source 1 (S1) on the right and source 2 (S2) on the left.

3. Results and Discussion

The results of the measurement of the samples composed of loose olive wood chips used as a filler material inside birch plywood frames are first analyzed in this section, and the effects the TNT and spray film coating had on the values are highlighted. In order to assess the quality of absorption and to provide designers and architects with a simplified and quick method to evaluate the sound absorption performance of individual products, the value of the weighted sound absorption coefficient (α_w) is given in commercial data sheets but, in this paper, it was calculated for the configurations defined in Section 2.2.1 as a single, purely comparative value, as anticipated in Section 2.

It should be pointed out that a good match of results was shown in the frequency range above 400 Hz in [17], but greater mismatches can occur at low frequencies because of the small size of the room. Thus, the colored band represented in each graph below indicates the frequency below which absorption values are considered less accurate (f = 400 Hz). However, a relative comparison between samples is also possible below this frequency.

3.1. Different Pattern Configuration for Exposed Porous Material

The graphs in Figures 11–13 show the values obtained from the SSRR measurements of the configurations presented in Figure 5, for a reference area of 0.27 m^2.

First, the comparison of the sound absorption curves of the acoustically hard BASE, the Pattern-B acoustically hard empty (B_{empty}), and the full of olive tree pruning chip (B_{full}) configurations is shown, with the purpose of highlighting the influence of the porous material on the frequency absorption. In fact, the absorption values increased from 0.25 for the B_{empty} sample to 0.50 for the B_{full} sample, at a maximum of 1600 Hz, while the minimum increased from 0.05 to 0.15 at 3150 Hz, and from 0.10 to 0.45 at 4000 Hz, respectively. The porous material thus contributed significantly to the improvement of the acoustic behavior of the samples and led to an increase in the absorption coefficient for the maxima of 1600 Hz and above 4000 Hz, and for the minimum of 3150 Hz, by about 0.2 points on average.

The B_{empty} configuration showed a significantly higher peak over a narrow range of frequencies around the 1600 Hz third-octave band. This might be due to the resonant absorption [27] of the 200 mm and 100 mm empty boxes, which have limited internal dimensions of 188 mm and 88 mm, respectively. These are comparable to the wavelength ($\lambda \approx 210$ mm) and half-wavelength of the 1600 Hz third-octave band. The effect is similar to that observed for the absorption phenomenon that occurs for sound diffusers [27], where

resonant absorption occurs, due to the one-quarter wave resonances in the walls created by the box boundaries and the energy flow between the boxes.

The effect induced by the boxes also broadened the maxima of the first resonant frequency related to the quarter-wavelength (i.e., 2257 Hz, which falls into the 2500 Hz third-octave band), including the 1600 Hz peak. This effect is evident when comparing the BASE, B_{empty}, and B_{full} configurations. It should be highlighted that the effect is also maintained for the B + $O100l_{full}$ and $O100l_{full}$ configurations, where larger boxes (300 × 300 mm) were used for the O100l samples. The 3150 Hz trough results were slightly influenced by the different configurations, resulting in a decrease in the sound absorption coefficient. It is possible to hypothesize that the visco-thermal losses that take place within the material are not sufficient to completely absorb the sound wave at this specific wavelength.

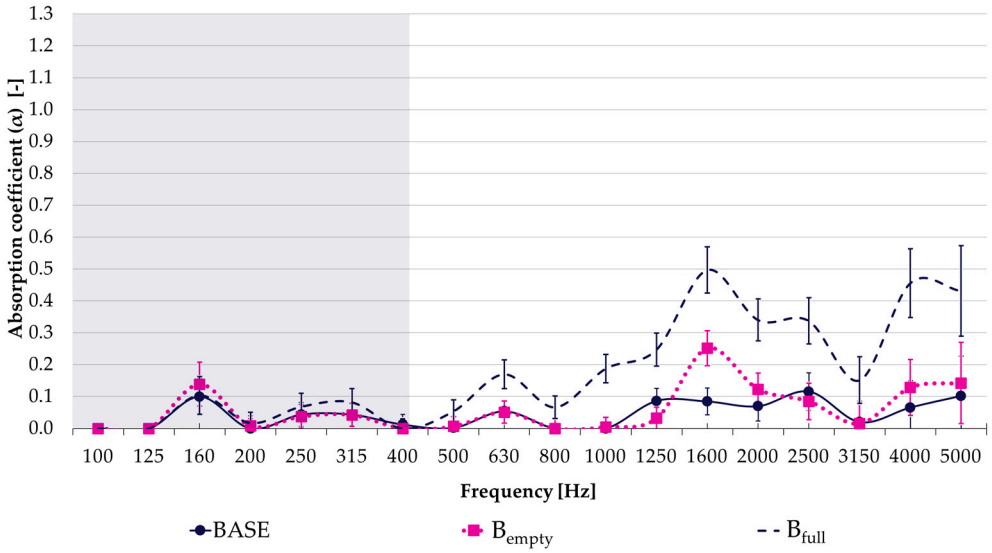

Figure 11. The obtained random incidence sound absorption coefficients of the BASE, B_{empty}, and B_{full} configurations, together with the standard deviations of the results for each sample configuration.

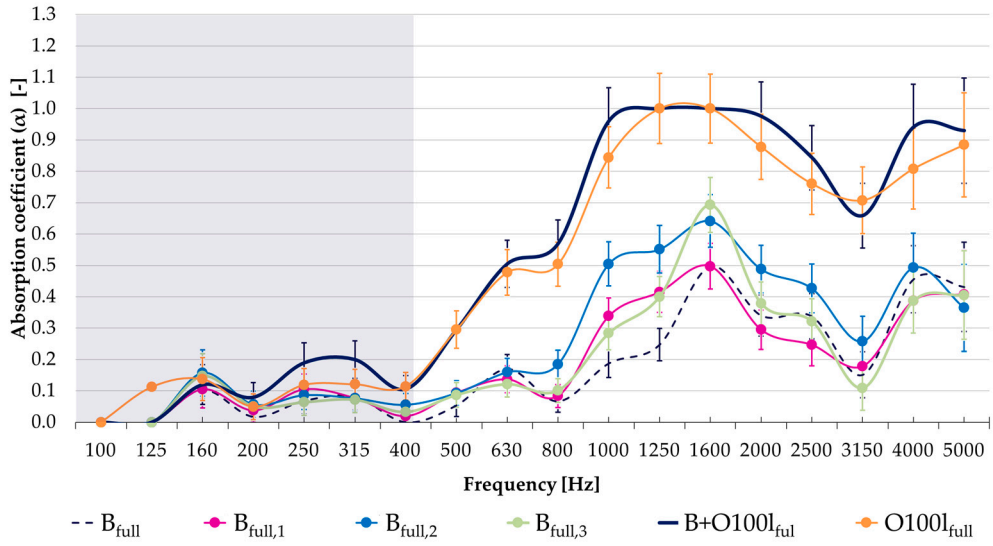

Figure 12. The obtained random incidence sound absorption coefficients of the B_{full}, $B_{full,1}$, $B_{full,2}$, $B_{full,3}$, B + $O100l_{full}$, and $O100l_{full}$ configurations, together with the standard deviations of the results of each sample configuration.

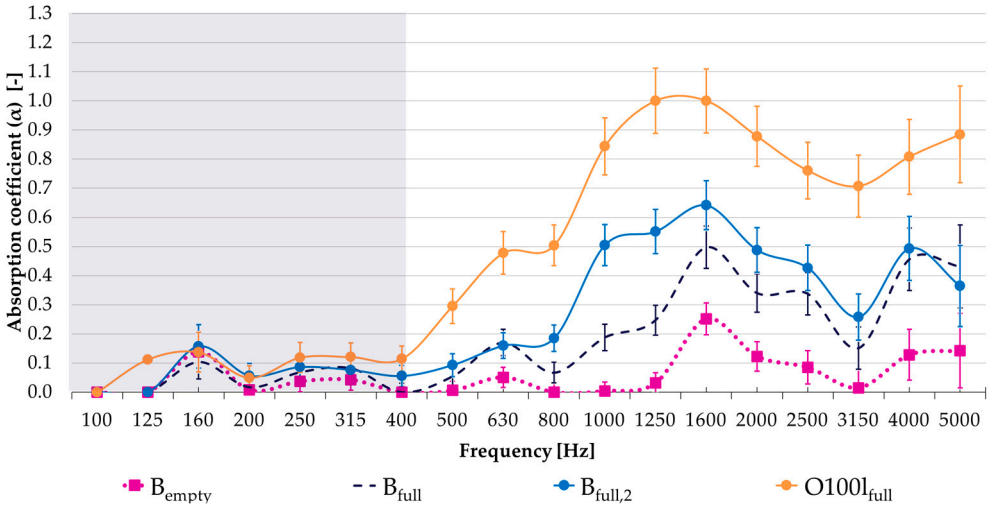

Figure 13. The obtained random incidence sound absorption coefficients of the B_{empty}, B_{full}, $B_{full,2}$, and $O100l_{full}$ configurations, together with the standard deviations of the results of each sample configuration.

Next, the five configurations were compared with respect to the B_{full} sample, and the $B_{full,1}$, $B_{full,2}$, and $B_{full,3}$ configurations also showed lower absorption values—due to the diffraction effect of the underlying plywood panel, and to the smaller exposed sound-absorbing surface area (0.09 m^2 out of 0.27 m^2 total)—than the B + $O100l_{full}$ and $O100l_{full}$ configurations (0.27 m^2 out of the total 0.27 m^2). The curves show that the modules and their arrangement make this solution flexible, both aesthetically and in terms of sound absorption; in fact, each configuration obtained a different curve with absorption values that on average were between 0.35 and 0.90 in the mid-high frequencies, but the maxima were kept at frequencies of 1600 Hz and 4000 Hz, and the minimum at 3150 Hz. However, the values could be improved by introducing a greater thickness.

In short, it is possible to state that a lower absorption at lower frequencies is characteristic of the porous material, with values of more than 0.3 from 500 Hz onward for compositions with the total full exposed area (0.27 m^2); the same value was obtained by Martellotta et al. [14] from 400 Hz onward. Another characteristic of this material is the constant recording of peaks, for any configuration, at about 1600 Hz and at 4000 Hz, with values of between 0.50 and 1. Thus, a correspondence of the frequency values recorded in [14] can be noted, but with a small variation, at 1200 Hz, with 0.55, and at 4000 Hz with 0.95, although only olive leaves were considered in that work. The present results differ from those obtained in [14] concerning the minimum, which, in this research, is at 3150 Hz, rather than 2000 Hz. In agreement with previous studies on loose material [14], the peaks show a shift towards lower frequencies, when compared with the theoretical frequency (i.e., quarter-wavelength f_0 = c/4d, where c = 343.1 m/s at 20 °C) for hard backed porous material, which, in this case, was estimated to fall within the 2500 Hz third-octave band.

Moreover, the slight differences between the B + $O100l_{full}$ and $O100l_{full}$ samples might be due to the fact that, although these samples apparently had the same degree of compaction (the particles were poured and shaken in a similar way), the position and orientation of the particles might have been slightly different. As shown in [28], the compaction degree of the chips can also have a significant effect on the translation of the peaks.

Finally, the configurations studied in the following sections, that is, $B_{full,2}$ and $O100l_{full}$, were compared, with respect to the influence of TNT and the spray film coating, with Empty Pattern-B (B_{empty}) and Full Pattern-B (B_{full}).

Figure 14 shows the weighted sound absorption values: α_w. Through these comparisons, it is even more evident that patterns or configurations can be shaped according to the needs of the individual user and the intended use of the rooms. The α_w coefficient increases

from 0.05 (acoustically hard) for the BASE and B_{empty} configurations, to $\alpha_w = 0.15$ for the B_{full} configuration. $B_{full,1}$ and $B_{full,3}$ also obtained an $\alpha_w = 0.15$. The best performance was obtained for $B_{full,2}$, with a value of $\alpha_w = 0.20$, and for B + O100l$_{full}$ and O100l$_{full,}$ with a value that reached $\alpha_w = 0.35$, but for a larger effective absorbing area. It can therefore be seen that the configurations of the sub-modules are absorbing.

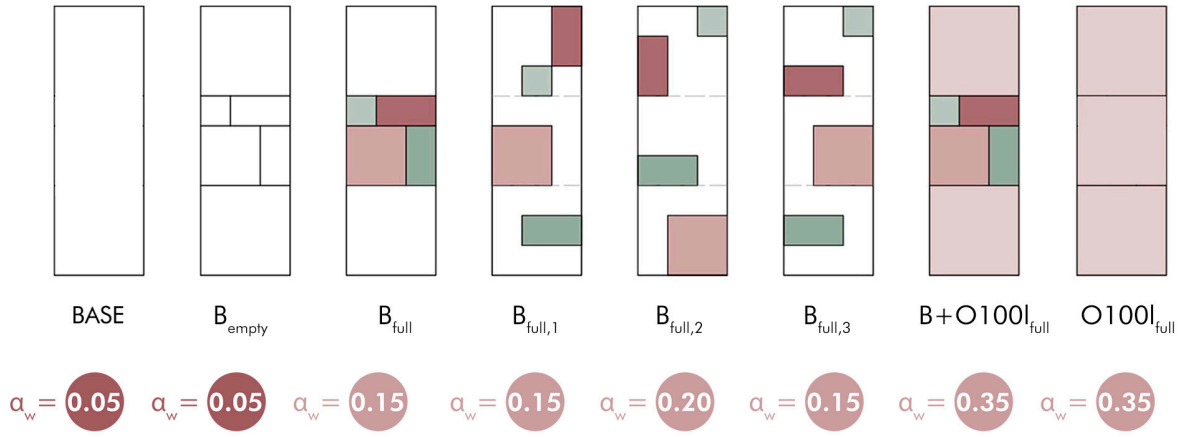

Figure 14. Weighted sound absorption coefficient of the various configurations presented in Figure 5.

The variety of patterns shows a high flexibility and would allow designers to obtain a more efficient use of absorbing materials, that is, by combining the acoustic performance with the aesthetic performance of the final panel.

Moreover, the correspondence of the peaks with the characteristic geometrical dimensions of the sample patterns was verified (Table 2): (1) in relation to the thickness of the loose material d = 38 mm which corresponds to the quarter-wavelength resonance frequency (f_0 = c/4d) of 2257 Hz and falls within the 2500 Hz third-octave band; (2) in relation to the length (l = 188 mm) and width (w = 88 mm) of the boxes a frequency of 456 Hz and 974 Hz, respectively, which refer to the quarter-wavelength resonance frequencies, and these wavelengths fall within the 500 and 1000 Hz third-octave bands; (3) the largest inner dimension (l = w= 288 mm), which is characterized by a frequency a frequency of 298 Hz, corresponding to the longest wavelength, and falls within the 315 Hz third-octave band. Interestingly, some of these frequencies could show an evident relationship with the peaks of the sound absorption curves.

Table 2. Evaluation of the wavelengths in relation to the dimensions of the sample elements. The inner dimensions of the boxes are indicated in bold. λ is the wavelength corresponding to the third-octave band f when $d = \lambda/4$.

Sample Elements Dimensions	**Corresponding Quarter Wavelength Resonance Frequency**	***f* [Hz]**		
***d* [mm]**	**f_0 [Hz]**	**λ/4**	**λ/2**	**λ**
300	286	315	630	1250
288	**298**	**315**	**630**	**1250**
200	429	400	800	1600
188	**456**	**500**	**1000**	**2000**
100	858	800	1600	3150
88	**974**	**1000**	**2000**	**4000**
38	**2257**	**2500**	**5000**	**-**

3.2. The Effect of the TNT Application

Another measurement was conducted in the SSRR, with the aim of comparing the frequency data of the sample with exposed wood chips with the sample with TNT to see whether the latter could affect the acoustic properties of the modules. The graph in Figure 15 summarizes the results obtained for the two measurements.

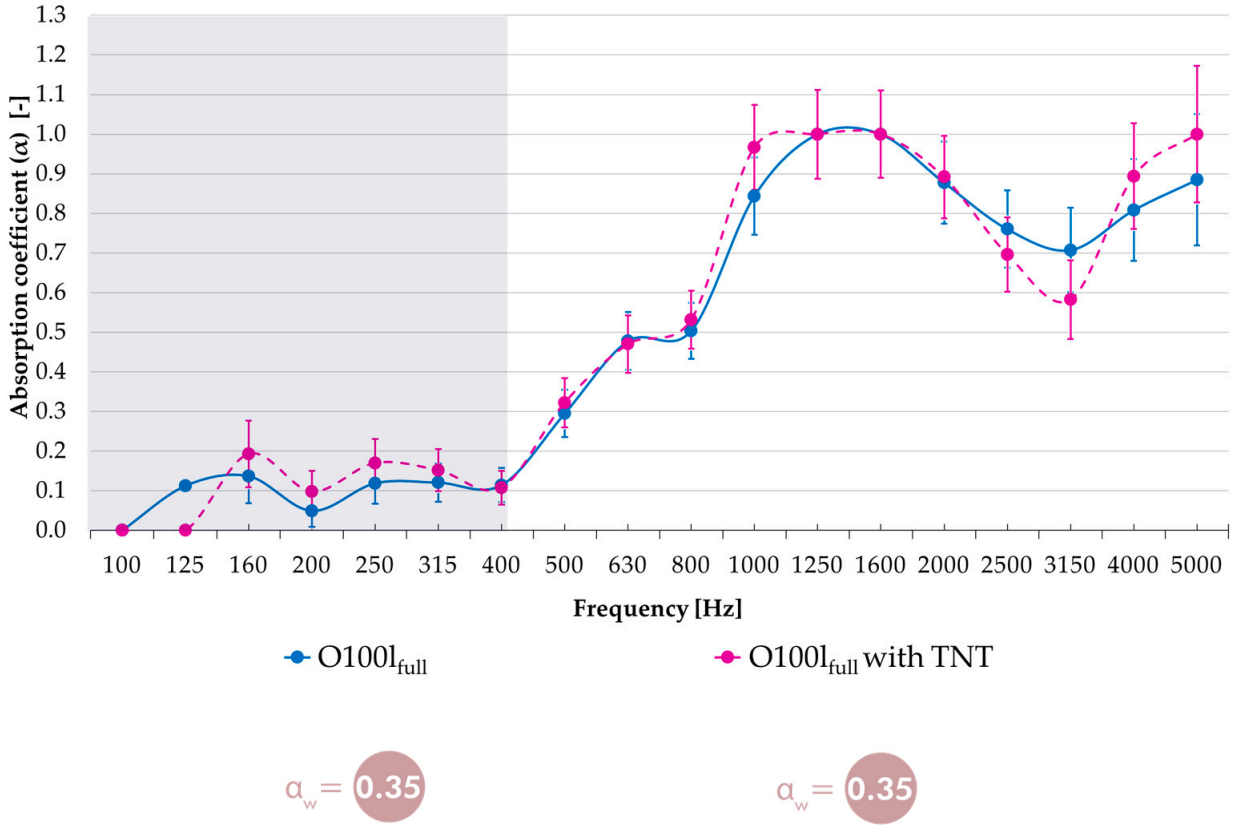

Figure 15. The obtained random incidence sound absorption coefficients from O100l$_{full}$ and O100l$_{full}$ with TNT and the standard deviations.

The results are compatible, and the use of TNT (Figure 7b) resulted in a further decrease in the minimum at 3150 Hz from 0.70 to just under 0.60, but also in a switch above 3150 Hz with higher absorption values than in the sample without the TNT (Figure 7a). However, even in this case, the values of α_w are 0.35.

3.3. Influence of the Spray Film Coating Application

As described in Section 2.2.2., a film-forming spray was used to fix the material within the frames and to be able to visualize the analyzed material. A new measurement of $B_{full,2}$ configuration was started in the SRR for this purpose, after the application of the spray.

This test demonstrated that the frequency trend of the curves with the spray (Figure 9b) and without the spray (Figure 9a) is compatible (see Figure 16). As expected, the spray did not close the open pores between the chips, and did not alter the acoustic behavior of the panels that had the same α_w values, that is, equal to 0.20, and maintained the maxima at 1600 Hz and 4000 Hz, and the minimum at 3150 Hz, with values between 0.3 and 0.6.

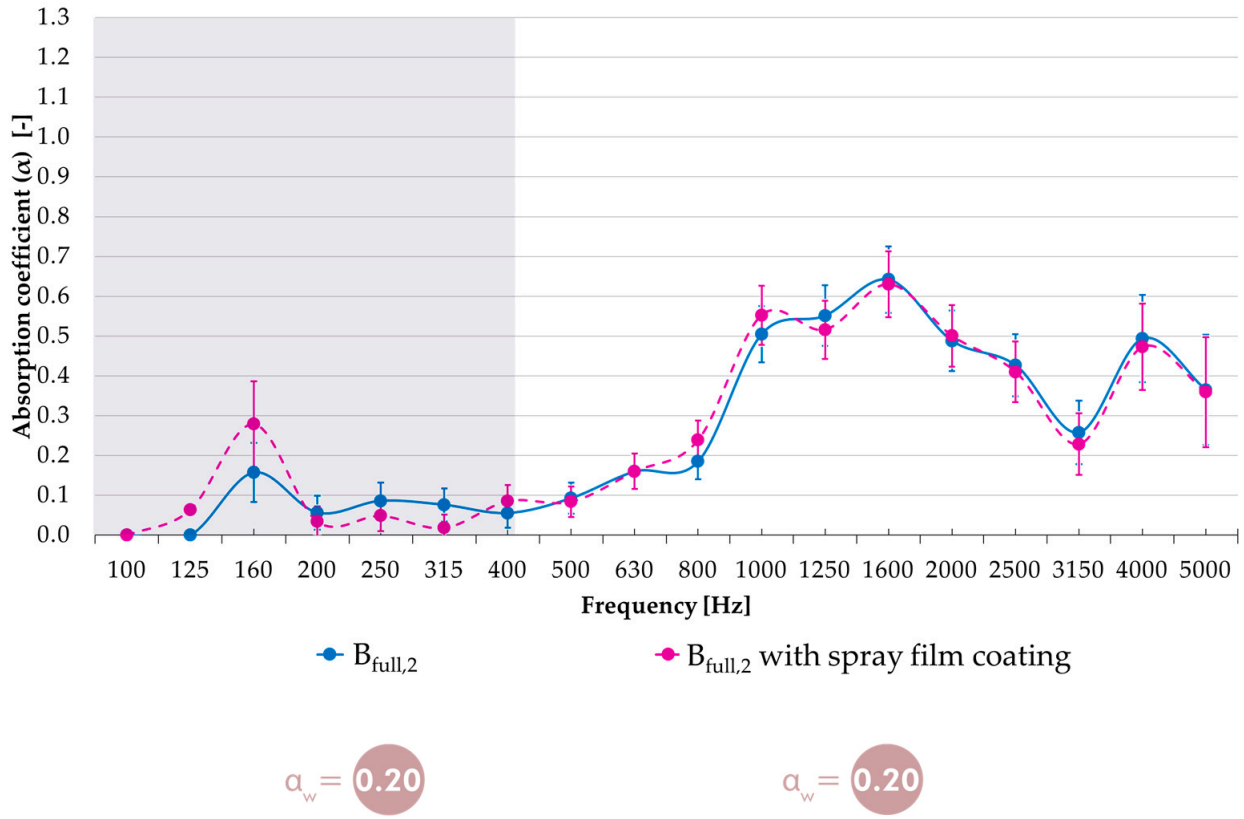

Figure 16. The obtained random incidence sound absorption coefficients from $B_{full,2}$ and $B_{full,2}$ with the spray film coating and the standard deviations.

4. Conclusions

Olive tree pruning chips were used in this work as a renewable resource to produce an environmentally friendly sound-absorbing material, and to promote the reuse of agricultural waste pruning. Six different specimen configurations, each composed of a frame and binder-free loose wood chips, were studied by varying the position of the specimens on the floor of a small-scale reverberation room (SSRR) to investigate the variation of the absorption in the diffuse field. All the configurations with the porous absorbent material in the cavity showed absorption values from above 800 Hz, with the maxima at 1600 Hz and 4000 Hz, and the minimum at 3150 Hz.

The results and the behavior of the curves are typical of the sound absorption coefficient of porous sound absorbing materials placed against a hard wall. They present a sound absorption coefficient, versus frequency, with a succession of peaks and troughs. It was noted that the sound absorption properties were higher at high frequencies than at low frequencies. A significant absorption coefficient (higher than 0.5) appeared above 800 Hz similarly for the B + $O100l_{full}$ and $O100l_{full}$ configurations. Moreover, significant maxima results appeared at around the 1600 Hz third-octave band for Pattern-B in different configurations, with a broader distribution over the adjacent frequencies for the $B_{full,2}$ configuration. This may be attributed to a combination of different factors related not only to the absorptive loose material, but also to an optimized distribution of the container boxes.

The two technological solutions adopted to improve the fixation of the loose material, namely, TNT and the spray film coating, did not influence the sound absorption values. In addition to showing a good sound absorption performance, the olive tree pruning wood chips showed important aesthetic qualities, as a result of their warm tones, which make the texture appealing for indoor environments.

This experimental study demonstrates the possibility of reusing olive tree pruning waste to produce innovative and sustainable sound-absorbing materials. Further investigations are underway to evaluate the thermal and hygrometric performances of the material.

In order to complete the analysis of the potential use of olive wood chips for acoustic applications in the architectural sector, panels with higher absorption areas and greater thicknesses, combined with perforated panels, could be further investigated to achieve a broader frequency absorption. In addition, the obtained samples have a wide range of uses, but other characteristics will be determined in future works. The fundamental properties of the material, i.e., flow resistivity, porosity, pore shape factor, tortuosity, etc., will be further evaluated to define an appropriate model for the prediction of sound absorption.

Author Contributions: Conceptualization, R.C., V.S., S.L.P. and L.S.; methodology, R.C., V.S., S.L.P. and L.S.; formal analysis, R.C. and L.S.; investigation, R.C.; data curation, R.C. and L.S.; writing—original draft preparation, R.C.; writing—review and editing, R.C., V.S., S.L.P. and L.S.; visualization, R.C.; supervision, V.S., S.L.P. and L.S. All authors have read and agreed to the published version of the manuscript.

Funding: This research received no external funding.

Institutional Review Board Statement: Not applicable.

Informed Consent Statement: Not applicable.

Data Availability Statement: Not applicable.

Acknowledgments: The authors would like to thank Andrea Bottega (Politecnico di Torino) for his support during the set-up preparation, DONNAFUGATA S.r.l. Agricultural Society for the olive tree pruning chippings, and Lg Parquet di Giuseppe Lombardo for the plywood waste for the frames.

Conflicts of Interest: The authors declare no conflict of interest.

References

1. Arenas, J.P.; Sakagami, K. Sustainable Acoustic Materials. *Sustainability* **2020**, *12*, 6540. [CrossRef]
2. Arenas, J.P.; Asdrubali, F. Eco-Materials with Noise Reduction Properties. In *Handbook of Ecomaterials*; Martínez, L.M.T., Kharissova, O.V., Kharisov, B.I., Eds.; Springer International Publishing: Berlin/Heidelberg, Germany, 2018; pp. 1–26. [CrossRef]
3. Asdrubali, F.; Schiavoni, S.; Horoshenkov, K.V. A Review of Sustainable Materials for Acoustic Applications. *Build. Acoust.* **2012**, *19*, 283–312. [CrossRef]
4. Berardi, U.; Iannace, G. Acoustic characterization of natural fibers for sound absorption applications. *Build. Environ.* **2015**, *94*, 840–852. [CrossRef]
5. Berardi, U.; Iannace, G.; Di Gabriele, M. Characterization of sheep wool panels for room acoustic applications. In Proceedings of the Fourth International Conference on the Effects of Noise on Aquatic Life, Dublin, Ireland, 10–16 July 2016; p. 15001. [CrossRef]
6. Bousshine, S.; Ouakarrouch, M.; Bybi, A.; Laaroussi, N.; Garoum, M.; Tilioua, A. Acoustical and thermal characterization of sustainable materials derived from vegetable, agricultural, and animal fibers. *Appl. Acoust.* **2022**, *187*, 108520. [CrossRef]
7. Ouakarrouch, M.; Bousshine, S.; Bybi, A.; Laaroussi, N.; Garoum, M. Acoustic and thermal performances assessment of sustainable insulation panels made from cardboard waste and natural fibers. *Appl. Acoust.* **2022**, *199*, 109007. [CrossRef]
8. Gumanová, V.; Sobotová, L.; Dzuro, T.; Badida, M.; Moravec, M. Experimental Survey of the Sound Absorption Performance of Natural Fibres in Comparison with Conventional Insulating Materials. *Sustainability* **2022**, *14*, 4258. [CrossRef]
9. Lim, Z.; Putra, A.; Nor, M.; Yaakob, M. Sound absorption performance of natural kenaf fibres. *Appl. Acoust.* **2018**, *130*, 107–114. [CrossRef]
10. Borlea (Mureşan), S.I.; Tiuc, A.-E.; Nemeş, O.; Vermeşan, H.; Vasile, O. Innovative Use of Sheep Wool for Obtaining Materials with Improved Sound-Absorbing Properties. *Materials* **2020**, *13*, 694. [CrossRef]
11. Yang, T.; Hu, L.; Xiong, X.; Petrů, M.; Noman, M.T.; Mishra, R.; Militký, J. Sound Absorption Properties of Natural Fibers: A Review. *Sustainability* **2020**, *12*, 8477. [CrossRef]
12. Arenas, J.; Del Rey, R.; Alba, J.; Oltra, R. Sound-Absorption Properties of Materials Made of Esparto Grass Fibers. *Sustainability* **2020**, *12*, 5533. [CrossRef]
13. Putra, A.; Khair, F.A.; Nor, M.J.M. Utilizing Hollow-Structured Bamboo as Natural Sound Absorber. *Arch. Acoust.* **2015**, *40*, 601–608. [CrossRef]
14. Martellotta, F.; Cannavale, A.; De Matteis, V.; Ayr, U. Sustainable sound absorbers obtained from olive pruning wastes and chitosan binder. *Appl. Acoust.* **2018**, *141*, 71–78. [CrossRef]

15. Fico, D.; Rizzo, D.; De Carolis, V.; Montagna, F.; Palumbo, E.; Corcione, C.E. Development and characterization of sustainable PLA/Olive wood waste composites for rehabilitation applications using Fused Filament Fabrication (FFF). *J. Build. Eng.* **2022**, *56*, 104673. [CrossRef]
16. Chen, Y.; Yuan, F.; Su, Q.; Yu, C.; Zhang, K.; Luo, P.; Hu, D.; Guo, Y. A novel sound absorbing material comprising discarded luffa scraps and polyester fibers. *J. Clean. Prod.* **2020**, *245*, 118917. [CrossRef]
17. Shtrepi, L.; Prato, A. Towards a sustainable approach for sound absorption assessment of building materials: Validation of small-scale reverberation room measurements. *Appl. Acoust.* **2020**, *165*, 107304. [CrossRef]
18. Kwon, M.; Remøy, H.; Bogaard, M.V.D. Influential design factors on occupant satisfaction with indoor environment in workplaces. *Build. Environ.* **2019**, *157*, 356–365. [CrossRef]
19. Cucharero, J.; Hänninen, T.; Lokki, T. Influence of Sound-Absorbing Material Placement on Room Acoustical Parameters. *Acoustics* **2019**, *1*, 644–660. [CrossRef]
20. Labia, L.; Shtrepi, L.; Astolfi, A. Improved Room Acoustics Quality in Meeting Rooms: Investigation on the Optimal Configurations of Sound-Absorptive and Sound-Diffusive Panels. *Acoustics* **2020**, *2*, 451–473. [CrossRef]
21. *ISO 354:2003*; Acoustics-Measurement of Sound Absorption in a Reverberation Room. International Organization for Standardization: Geneva, Switzerland, 2003.
22. Gendek, A.; Aniszewska, M.; Chwedoruk, K. Bulk density of forest energy chips. *Ann. Warsaw Univ. Life Sci.—SGGW Agric.* **2016**, *67*, 101–111.
23. Cousin, B.; Lekounougou, S.-T. Initial moisture content, bulk density, bulk porosity and desorption isotherm of wood chips from five species of the boreal forest. *Wood Mater. Sci. Eng.* **2021**, *16*, 229–236. [CrossRef]
24. Grioui, N.; Halouani, K.; Zoulalian, A.; Halouani, F. Experimental study of thermal effect on olive wood porous structure during carbonization. *Maderas. Cienc. Y Tecnol.* **2007**, *9*, 15–28. [CrossRef]
25. *ASTM C423-17:2017*; Standard Test Method for Sound Absorption and Sound Absorption Coefficients by the Reverberation Room Method. ASTM International: West Conshohocken, PA, USA, 2008; JCGM 100, "Evaluation of measurement data—Guide to the Expression of Uncertainty in Measurement".
26. ITA-Toolbox for MATLAB Developed at the Institute of Technical Acoustics at RWTH Aachen University. Available online: https://www.ita-toolbox.org/ (accessed on 4 December 2022).
27. Cox, T.J.; D'Antonio, P. *Acoustic Absorbers and Diffusers: Theory, Design and Application*; Taylor and Francis: New York, NY, USA, 2017.
28. Glé, P.; Gourdon, E.; Arnaud, L. Acoustical properties of materials made of vegetable particles with several scales of porosity. *Appl. Acoust.* **2011**, *72*, 249–259. [CrossRef]